ELSEVIER

Experimental Hematology

Experimental Hematology 2008;36:1035–1046

Isolation and characterization of CD146$^+$ multipotent mesenchymal stromal cells

Antonio Sorrentino[a], Manuela Ferracin[b], Germana Castelli[a], Mauro Biffoni[a], Giada Tomaselli[a], Marta Baiocchi[a], Alessandro Fatica[c], Massimo Negrini[b], Cesare Peschle[a], and Mauro Valtieri[a]

[a]*Department of Hematology, Oncology, and Molecular Medicine, Istituto Superiore di Sanità, Rome, Italy;* [b]*Department of Experimental and Diagnostic Medicine and Interdepartmental Center for Cancer Research, University of Ferrara, Ferrara, Italy;* [c]*Institute Pasteur Cenci-Bolognetti, Department of Genetics and Molecular Biology, University of Rome ''La Sapienza,'' Rome, Italy*

(Received 29 October 2007; revised 10 March 2008; accepted 10 March 2008)

Mesenchymal stromal cells (MSCs) represent a bone marrow (BM) population, classically defined by five functional properties: extensive proliferation, ability to differentiate into osteoblasts, chondrocytes, adipocytes, and stromal cells—supporting hematopoiesis. However, research progress in this area has been hampered by lack of suitable markers and standardized procedures for MSC isolation. We have isolated a CD146$^+$ multipotent MSC population from 20 human BM donors displaying the phenotype of self-renewing osteoprogenitors; an extensive 12-week proliferation; and the ability to differentiate in osteoblasts, chondrocytes, adipocytes, and stromal cells supporting hematopoiesis. Furthermore, the CD146$^+$ MSCs secrete a complex combination of growth factors (GFs) controlling hematopoietic stem cells (HSCs) function, while providing a >2-log increase in the long-term culture (LTC) colony output in 8-week LTC over conventional assays. The hematopoietic stromal function exhibited by the MSCs was further characterized by manipulating LTCs with the chemical inhibitors Imatinib or SU-5416, targeting two GF receptors (GFRs), KIT or VEGFR2/1, respectively. Both treatments similarly impaired LTC colony output, indicating key roles for these two GF/GFR interactions to support LTC-initiating cell activity. CD146$^+$ MSCs may thus represent a tool to explore the MSC-HSC cross-talk in an in vitro surrogate model for HSC "niches," and for regenerative therapy studies. In addition, the MSC microRNA (miRNA) expression profile was analyzed by microarrays in both basic conditions and chondrogenic differentiation. Our analysis revealed that several miRNAs are modulated during chondrogenesis, and many of their putative targets are genes involved in chondrogenic differentiation.

Mesenchymal stromal cells (MSCs) represent a bone marrow cell (BM) population, classically defined by the ability to undergo sustained proliferation and the potential to give rise to multiple mesenchymal cell lineages, including osteocytes, chondrocytes, adipocytes, and reticular stromal cells supporting hematopoiesis [1–11]. In the mouse, MSCs have been isolated from virtually all postnatal murine organs and tissues, possibly due to their presence in a perivascular MSC niche [12]. In humans, MSC have been isolated from bone marrow [1–3,13], cord blood [13], adult peripheral blood, mobilized [14], or not [15], and adipose tissue [13]. A variety of heterogeneous MSC populations have been reported to possess additional functional properties, such as quasi-immortality [16], ability to homotypically differentiate into other mesodermic tissues as endothelium [17], astrocytes [18], myoblasts [19], or cardiomyocytes [20], and the capacity to heterotypically differentiate into neurons [21] and hepatocytes [18,22]. These reports utilized either human unseparated adherent mononuclear cells (MNCs) or different separation procedures, due to lack of consensus on the MSC phenotype. Recent studies indicated as putative MSC markers stage-specific embryonic antigens (SSEA-1 or -4) [18,23], neural ganglioside GD2 [24], or, most recently, CD146 [10,25]. This complex and somewhat contradictory scenario led us to develop a strategy to isolate homogeneous multipotent MSCs from human adult BM.

Offprint requests to: Mauro Valtieri, M.D., Department of Hematology, Oncology and Molecular Medicine, Istituto Superiore di Sanità, Viale Regina Elena 299, 00161 Rome, Italy; E-mail: valtieri@iss.it

0301-472X/08 $–see front matter.
doi: 10.1016/j.exphem.2008.03.004

We have enriched for a lin^- MNC-BM fraction, which was then $CD34^+$ cell−depleted and expanded in selective clonal/low-density adherent cultures, resulting in a $CD146^+$ MSCs population coexpressing 12 additional antigens, CD49a, CD90, CD105, CD140b, GD2, α-smooth muscle actin (α-SMA), alkaline phosphatase (ALP), but not the endothelial/hematopoietic CD31, CD34, CD45 markers. The $CD146^+$ MSCs extensively proliferate, differentiate in osteoblasts, chondrocytes, adipocytes, and efficiently support hematopoiesis in 8-week long-term culture (LTC), through a complex adhesion molecules expression and cytokine secretion pattern, including vascular endothelial growth factor (VEGF)-A/C, placental-derived growth factor, angiopoietin (Ang)-1/2, FLT-3 ligand (FL), stem cell factor (SCF) in both soluble and membrane-bound (mb) isoforms, bone morphogenetic protein (BMP) 2, stromal cell−derived factor 1 (SDF-1), interleukin (IL)-3, and granulocyte macrophage (GM-CSF)/macrophage colony-stimulating factor (M-CSF).

Finally, we have analyzed expression of microRNAs (miRNAs) in the $CD146^+$ MSCs and their chondrogenic progeny. miRNAs are small (~22 nt) single-stranded noncoding RNAs that serve as posttranscriptional regulators of gene expression, mainly by base-pairing to the 3′-UTR of target mRNAs, thereby causing translational repression and/or mRNA degradation [26]. To date, several hundred miRNAs have been discovered in a variety of organisms, playing a key role in basic cell functions (e.g., proliferation, differentiation, apoptosis) in both normal and pathological conditions [27]. We describe the MSC miRNA expression profile, analyzed by microarrays in either basal conditions or chondrogenic differentiation, showing a marked modulation of 36 miRNAs during chondrogenesis.

Materials and methods

Enrichment of MSCs

BM from healthy donors was purchased from CAMBREX Poietics cell systems (Gaithersburg, MD, USA). BM samples were treated for 20 minutes at 20°C with RosetteSep human MSC enrichment cocktail (StemCell Technologies, Vancouver, BC, Canada) composed by CD3, CD14, CD19, CD38, CD66b, Glycophorin A tetrameric antibody (Ab) complexes crosslinking unwanted cells with red blood cells, diluted and centrifuged over Ficoll-Hypaque gradient for 25 minutes at 300*g*. Enriched cells were collected, washed, and treated with NH_4Cl (StemCell) for 10 minutes in ice to remove residual red blood cells. $CD34^+$ cells were removed by MACS column (Miltenyi, Bergisch Gladbach, Germany). Enriched or unseparated cells were then cultured at clonal/low density (1−10 cells/cm^2) for 3 weeks in α-medium (Invitrogen, Carlsbad, CA, USA), 20% fetal calf serum (FCS; StemCell) in T75 flasks at 37°C in 5%CO_2 atmosphere. Half medium was replaced two times a week until MSCs reached confluence, defined as passage (P) 0. MSCs were detached by trypsin-ethylenediamine tetraacetic acid solution (Invitrogen) treatment and replated. Each weekly replating or P was defined by a progressive number.

MSC phenotyping

All Abs were purchased from BD Biosciences (San Diego, CA, USA). Senescence was evaluated by β-galactosidase staining kit (Cell Signalling, Beverly, MA, USA, http://www.cellsignal.com). MSC phenotype was analyzed by flow cytometry using a FACScan instrument (BD). Cell-sorting experiments were performed using a FACSaria instrument (BD).

LTCs

The 3.6×10^4 $CD146^+$ MSCs/cm^2 or 6.0×10^5 adherent cells derived from unseparated BM MNCs/cm^2 were seeded in 24-well/plates (Falcon) in α-medium, 20% MCS selected FCS; plates were then irradiated (2000 cGy) with a cesium source, and the medium changed to α-medium consisting of 10% FCS, 10% Horse S (both from StemCell Technologies, Vancouver, BC, Canada), and 10^{-6}M hydrocortisone (Sigma, St Louis, MO, USA) [28,29]. Plates were then seeded with $3 \times 10^3$$CD34^+$CB cells and cultured up to 8 weeks at 33°C in 5%CO_2 atmosphere. Half volume of each culture (.2 mL) was harvested weekly and replaced with fresh medium. Cells were then counted and seeded in multilineage semisolid medium for clonogenetic assay and replaced with fresh medium. In some experiments, the VEGFR2/1 chemical inhibitor SU5416 [30] (Sigma) was used at 1, 3, or 10 μM. SU5416 was added weekly with medium replacement. Equimolar amounts of Imatinib-mesylate (GLIVEC or ST1571) [31] (Novartis, Basel, Switzerland), a Kit inhibitor, were simultaneously added in control cultures. All experiments were performed in triplicate.

Clonogenetic cultures

Clonogenetic cultures [28,29] were prepared in Iscove's modified Dulbecco's medium (Invitrogen), 10% FCS, 10% Horse S (both from StemCell), 100 ng/mL SCF, FL, thrombopoietin, IL-3, GM-CSF, G-CSF, M-CSF, 3 U/mL erythropoietin (all from R&D Systems, Minneapolis, MN, USA); MTC 1.8% (StemCell). Suspension cells (100−400/dish) were seeded in triplicate 35-mm dishes and cultured for 2 weeks at 37°C in 5% CO_2, O_2 atmosphere.

MSC differentiation

Osteogenic. The 3.1×10^3 MSC/cm^2 were seeded in six-well/plates (BD) in MSCGM (Cambrex, Poietics Cell Systems) for 24 hours at 37°C in 5% CO_2 atmosphere. MSCGM was replaced with Osteogenesis Induction Medium (Cambrex), and MSCs cultured for 3 weeks with refeeding every 3 to 4 days.

Chondrogenic. The 2.5×10^5 MSC were washed twice at 150*g* for 5 minutes at 20°C with incomplete chondrogenic medium (Cambrex), resuspended in 0.5 mL complete medium (Cambrex) in 15 mL polypropylene tube and cultured for 3 weeks at 37°C in 5%CO_2 atmosphere, refeeding every 2 to 3 days with fresh medium.

Adipogenic. Confluent MSCs were supplemented with Adipogenesis induction medium for 3 days followed by 1 to 3 days of culture in Adipogenic maintenance medium (both from Cambrex). After three cycles of induction/maintenance, cells were cultured

for an additional week with Adipogenic maintenance medium replacing the medium every 2 to 3 days.

Cytokine measurement
Cytokine levels were analyzed by enzyme-linked immunosorbent assay kits according to the manufacturer's instructions (Quantikine, R&D).

Confocal immunofluorescence microscopy
MSCs were fixed in 0.4% paraformaldehyde−phosphate-buffered saline (Sigma-Invitrogen) for 20 minutes at 20°C, permeabilized in 0.2% Triton X-100, 1% bovine serum albumin (both from Sigma) in phosphate-buffered saline (Invitrogen), wash buffer (WB) for 15 minutes at 20°C, three times washed for 5 minutes with WB. Samples were incubated overnight at 4°C with α-SMA Ab (Sigma). The following day, samples were washed three times with WB, incubated with fluorescein isothiocyante−conjugated goat α-mouse IgG2a for 1 hour at 25°C, and then washed again. Nuclei were counterstained with TOTO3 (Molecular Probes, Invitrogen) and coverslides mounted. Images were collected with a laser scanning microscope (Olympus, Tokyo, Japan).

Western blot
Membrane proteins were extracted by incubating cells for 30 minutes at 4°C in a membrane isolation buffer (Tris [pH 7.4] 20 mM, ethylenediamine tetraacetic acid 2 mM, Na_3VO_4 0.2 M). Nuclei were discarded by centrifugation at 1000*g* for 5 minutes, and the membrane fraction was subsequently obtained by ultracentrifugation of the remaining solution at 30,000*g* for 30 minutes at 4°C. Membrane pellets were lysed using the CelLytic M Lysis Reagent (Sigma), with Protease Inhibitor Cocktail (Sigma) following manufacturer's protocol.

Abs used for immunodetection were anti-SCF (R&D), anti−β-actin (Chemicon, Temecula, CA, USA) and secondary anti-mouse IgG peroxidase conjugate (Pierce, Rockford, IL, USA).

Reverse transcriptase polymerase chain reaction
Total RNA was isolated by Trizol (Invitrogen) following manufacturer's instructions. First-strand cDNA was synthesized with SuperScript II (Invitrogen) using 1 μg total RNA for each sample and oligo(dT) (Invitrogen). Polymerase chain reaction was performed using the following primers:

mbSCF For 5′-CAGTGACCATCTACAGCTTTCCGG-3′
mbSCF Rev 5′-GCTGCTACCACAGTGATGATGACAA-3′
S26 For 5′-GGTCCGTGCCTCCAAGATGA-3′
S26 Rev 5′-AAATCGGGGTGGGGGTGTT-3′

miRNA microarray
Total RNA was extracted from two basal and two chondrogenic differentiated MSC cultures by Trizol (Invitrogen) according to manufacturer's instructions. One-color RNA labeling and hybridization on miRNA microarray chips were performed as described previously [32,33]. Briefly, 5 μg RNA from each sample were hybridized on a miRNA microarray consisting of 226 probes for human miRNAs. Hybridization signals were detected by biotin binding of a Streptavidin-Alexa 647 conjugate using a GenePix 4000B scanner (Axon Instruments, Sunnyvale, CA, USA). Images were quantified by the GenePix Pro 6.0 (Axon).

Analysis of microarray data
Raw data from one-color miRNA microarrays were normalized and analyzed by GeneSpring GX software version 7.3 (Agilent Technologies, Santa Clara, CA, USA). The GeneSpring software generated a unique value for each miRNA, performing the average of replicate probes present on the chip. Samples were normalized using the on-chip median normalization. Chondrocytes were normalized on basal MSCs and the miRNAs differentially expressed between the two populations were identified by using a filter based on a fold change of 1.3 combined with a Student's *t*-test ($p < 0.05$). Unsupervised hierarchical cluster analysis was performed after normalization procedures using average linkage and Pearson correlation as measure of similarity.

miRNA target prediction
Analysis of miRNA predicted targets was determined using the algorithms TargetScan (http://genes.mit.edu/targetscan) [34], PicTar (http://pictar.bio.nyu.edu) [35], and miRanda (http://cbio.mskcc.org/cgi-bin/mirnaviewer/mirnaviewer.pl) [36].

miRNA northern blot
RNA (4 μg) samples were run as described [32,33]. The oligonucleotides used as probes are:

miR-23a 5′ - AAATCCCATCCCCAGGAACCCC - 3′
miR-26b 5′ - ACCTATCCTGAATTACTTGAA -3′
Let-7a 5′ - AACTATACAACCTACTACCTCA - 3′
miR-214 5′ - GCACAGCAAGTGTAGACAGGCA - 3′
U2 5′ - GGGTGCACCGTTCCTGGAGGTAC - 3′

Results

Phenotyping of MSC
We have isolated a lin^- mononuclear BM cell fraction, which was then $CD34^+$ cell−depleted and expanded in clonal/low-density MSC culture (1−10 cells/cm^2): in this in vitro condition, the proliferating $CD146^+$ colony-forming unit fibroblast (CFU-F) clones (Suppl. Fig. 1C, right microphotograph) became prevalent after 2 weeks of culture over committed contaminating cells and finally merged after 3 weeks, defined as P0 (Fig. 1). $CD146^+$ cells in crude BM-MNC fractions, including $CD34^+$ endothelial cells, were under the detectability level (∼0.1%) (Suppl. Fig. 1A) [10], but they were enriched ∼10 to 15 times after our negative selections (Suppl. Fig. 1B). The preliminary selections of the uncultured cells were also critical for the homogeneity of the final $CD146^+$ MSCs population because in parallel crude BM-MNC expansions ≥30% contaminating CD31, CD34, and CD45 cells were detected (not shown). Lin^- $CD34^-$ BM MNCs cultured in 20% FCS preselected for MSCs growth at clonal/low-density, progressively expanded the $CD146^+$MSCs to homogeneity in 3 weeks (P0) (Fig. 1), while former studies with crude BM MNCs reported a ∼15% level of expression of CD146 in similar culture conditions [25]. Cell-sorting experiments, performed before the $CD146^+$ cells became homogeneous (P −1) (Suppl. Fig. 1C) confirmed that the fraction generating CFU-F (Suppl.

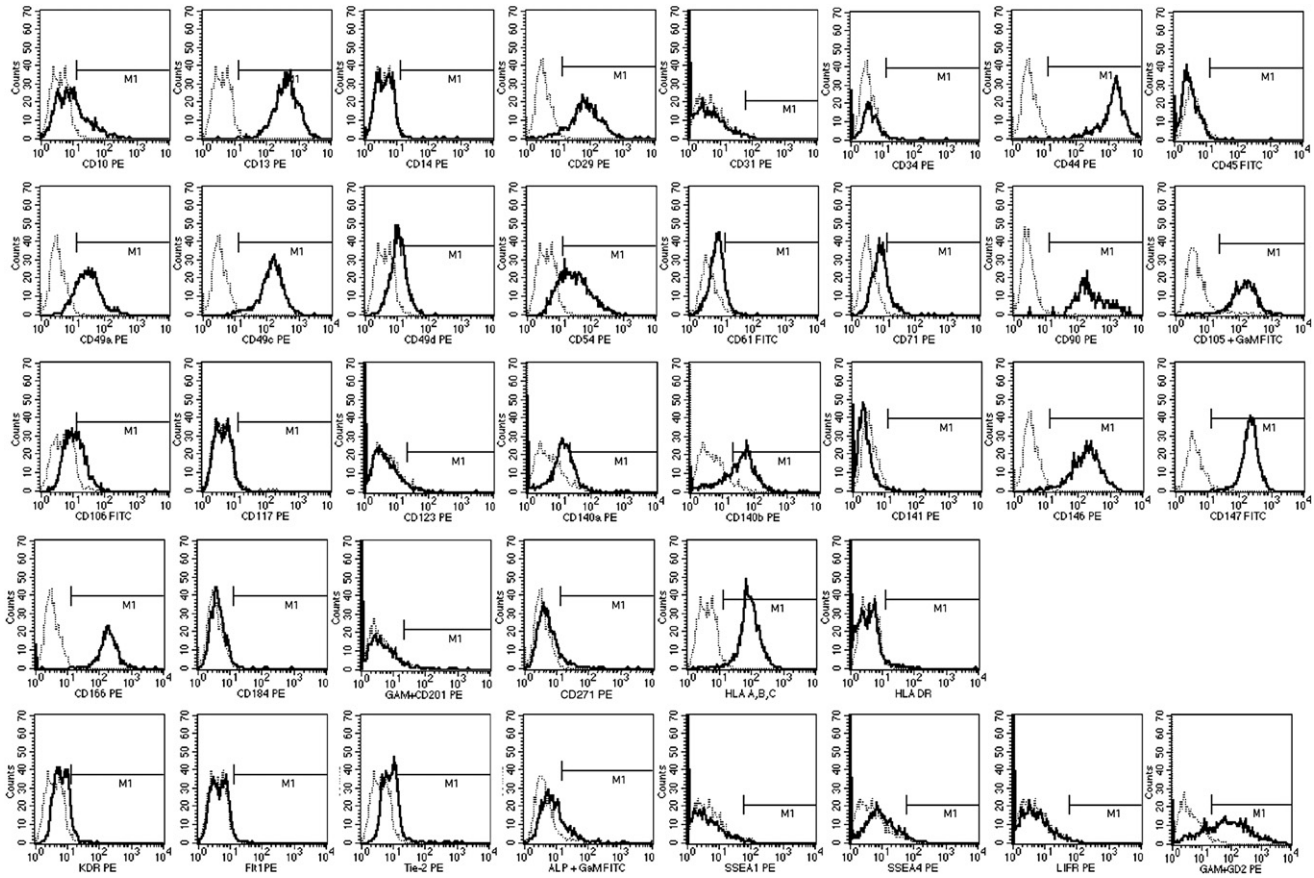

Figure 1. MSC antigen expression. Flow cytometry analysis of hematopoietic, endothelial, and stromal membrane antigens on homogeneous MSC populations. Several adhesion molecules and growth factor receptors are expressed. FITC = fluorescein isothiocyanate; PE = phycoerythrin.

Fig. 1C, right microphotograph) and proliferating up to 13 additional weeks was CD146$^+$, while CD146$^-$ cells could be barely maintained for 2 weeks (Suppl. Fig. 1C, left microphotograph). The isolation method used led to a consistent yield of homogeneous CD146$^+$ MSCs for all 20 BM isolations that were phenotyped using a panel of 39 monoclonal Abs against hematopoietic, endothelial, or stromal antigens (Fig. 1). Among the hematopoietic markers, including several adhesion proteins, some were expressed by all MSCs at high (CD13/Aminopeptidase N, CD29/β1-integrin, CD44/H-CAM, CD49a/α1-integrin, CD49c/α39-integrin) or low-intensity (CD49d/α49-integrin, CD10/CALLA, CD61/β3-integrin), while others were negative (CD45, CD14, CD31/PECAM1, CD34, CD117/KitR). MSC also showed several antigens usually expressed by endothelial cells at either high (CD105/TGFβR, CD146/S-endo/melanoma cell adhesion molecule [10,25], CD147/neurothelin, CD166/ALCAM) or lower intensity (CD54/ICAM1, CD106/vascular cellular-adhesion molecule 1 [VCAM1]). Among endothelial growth factor (GF) receptors, Kinase domain receptor/VEGFR2 and Tie-2/Angpt1-2R were weakly expressed whereas CD141/thrombomodulin, CD184/CXCR4 and Flt-1/VEGFR1 were below detection level. The stromal marker CD90 and the recently described MSC marker, GD2 [24] were highly expressed, as observed for CD140b/platelet-derived growth factor receptor (PDGFR) β [37,38] and to a lesser extent CD140a/PDGFRα [37,38]. α-SMA was significantly expressed and mostly organized in fibers (Fig. 2K) [39] indicating the potential for myoblastic differentiation. Conversely, ALP, CD271/nerve growth factor receptor, and SSEA4 [23] were expressed at lower levels, while SSEA1, a marker for pre-MSCs [18], was almost undetectable (Fig.1). CD71/TrfR expression is apparently linked to the presence of an actively proliferating fraction. HLA-ABC/major histocompatibility complex class I expression was high (99.3%) while HLA-DR/major histocompatibility complex class II, and leukemia inhibitory factor receptor were low (Fig.1). Altogether, our CD146/CD105/CD140b/CD49a/ALP/α-SMA$^+$, CD31/CD34/CD45$^-$ MSC phenotype is consistent with the recently described proliferating CFU-F, termed *adventitial reticular cell* or hematopoiesis-supporting stromal cell [10]; furthermore, the MSC phenotype analysis has been extended to other markers up to a total of 39 antigens.

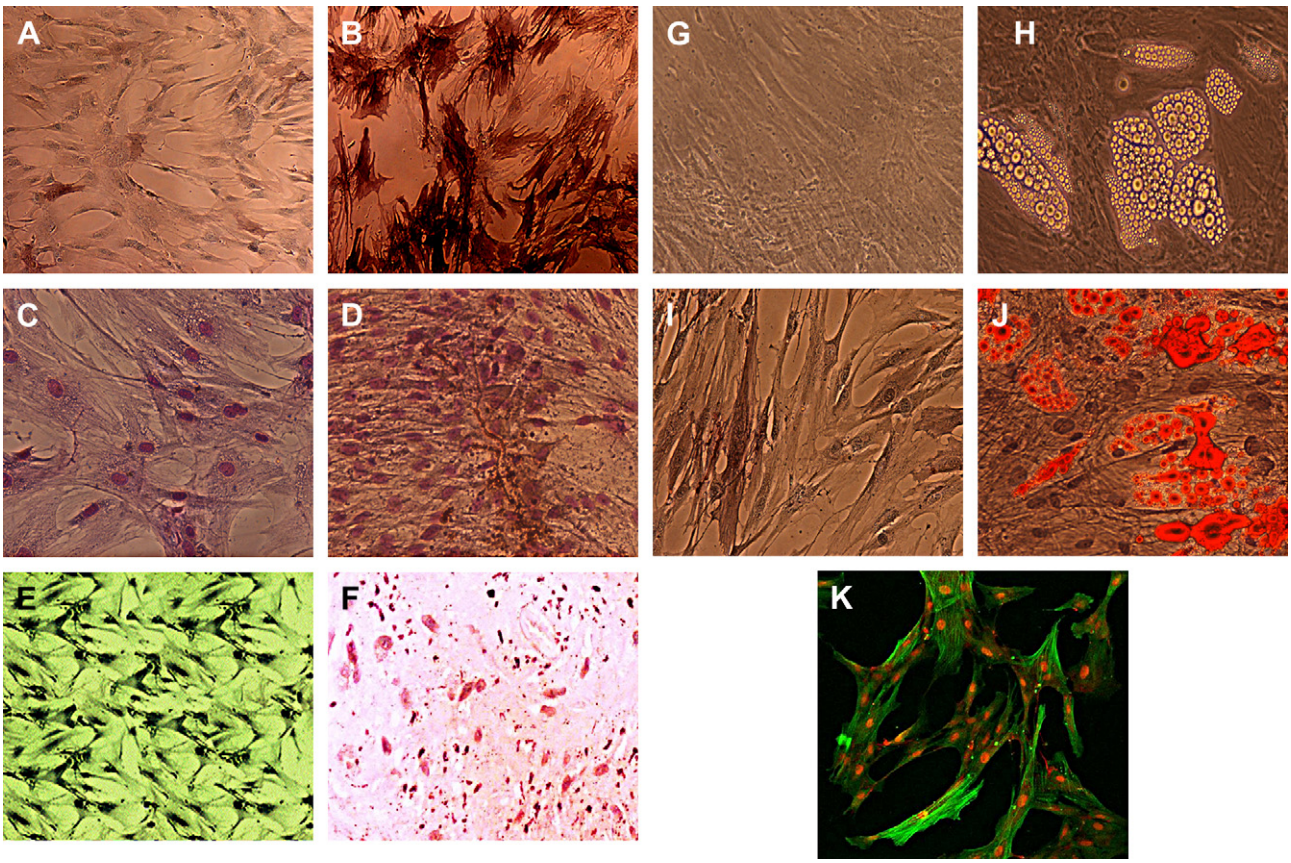

Figure 2. (**A**) ALP staining in undifferentiated MSCs and (**B**) osteogenic-induced MSCs after 1-week culture (30×). (**C**) Von Kossa staining for calcium deposition in undifferentiated MSCs and (**D**) in differentiated MSCs after 3-week osteogenic culture (May-Grünwald/Giemsa counterstain, 60×). (**E**) Safranin O staining in undifferentiated MSCs (60×) and in differentiated MSCs after 3 week chondrogenic culture (**F**) (30×). (**G**) Undifferentiated MSC and (**H**) adipogenic 4-week differentiation of MSCs (phase contrast, 30×). (**I**) Oil Red staining of undifferentiated MSCs and (**J**) in differentiated MSCs after 4 week adipogenic culture (60×). (**K**) MSCs express fibrillar smooth muscle actin. Cells were stained by immunofluorescence with anti-smooth muscle actin (SMA). Confocal laser scanning images are shown (60×).

MSC proliferation

MSCs could be expanded up to 12 weeks (P12), showing a progressively decreasing proliferation rate. Doubling time was 84 hours from weeks 0 to 4, 168 hours from weeks 4 to 8, 336 hours from weeks 8 to 12, correlating with the decrease of proliferating $CD71^+$ MSCs. By week 12, virtually all the MSCs stained positive for β-Gal (Suppl. Fig. 1), indicating an arrested state or senescence [40]. The antigen expression pattern was relatively stable up to P12 for 20 of the monitored markers. CD141 modestly increased from P1 to P9 while the remaining 18 monitored markers decreased over time (Suppl. Fig. 2). Interestingly, the multilineage $CD146/MCAM^+$ population sharply decreased at P10 in parallel with a drop of the proliferation rate.

MSC multilineage differentiation

When cultured in proper differentiation medium, $CD146^+$ MSCs differentiated not only in osteoblasts or HSC-supporting cells [10], but also toward chondrocytes and adipocytes [25].

Osteoblasts. MSCs are largely positive for ALP after 7 days (Fig. 2 A,B) and present typical calcium deposition, as revealed by Von Kossa staining, after 21 days of osteogenic differentiation (Fig. 2 C,D).

Chondrocytes. MSCs induced in chondrogenic differentiation for 3 weeks are shown after Safranin O staining (Fig. 2 E,F).

Adipocytes. MSCs induced in adipogenic differentiation for 4 weeks are shown in phase contrast (Fig. 2 G,H) and after oil red O staining (Fig. 2 I,J).

Cytokine production by MSC

$CD146^+$ MSC cytokine secretion was analyzed for 16 GFs (Table 1). Among the hematopoietic growth factors, FL, IL-3, GM-CSF, and M-CSF, were abundantly produced, while little soluble SCF was secreted. However, mbSCF was easily detected by reverse transcriptase polymerase chain reaction performed using isoform-specific primers and by

Table 1. Cytokine production by mesenchymal stromal cell

	Mean ± SEM (pg/mL/10^5 cells/24 hours)	No. of experiments
Flt-3 ligand	67.3 ± 18.1	11
SCF	2.3 ± 1.8	12
IL-3	37.5 ± 6.9	8
GM-CSF	14.6 ± 4.5	9
M-CSF	125.9 ± 44.5	17
VEGF-A	625.8 ± 59.1	19
PlGF	24.1 ± 4.4	18
VEGF-C	1231.7 ± 196.0	7
VEGF-D	Neg	3
Angpt-1	510.0 ± 84.8	23
Angpt-2	87.0 ± 16.8	23
SDF-1	1147.7 ± 310.2	10
BMP-2	53.6 ± 14.4	9
BMP-4	Neg	9
LIF	Neg	9
IGF-1	Neg	8

Dosages of cytokines were performed using enzyme-linked immunosorbent assay kits according to manufacturer's instructions.
Angpt = angiopoietin; BMP = bone morphogenetic protein; GM-CSF = granulocyte macrophage colony-stimulating factor; IGF-1 = insulin-like growth factor 1; IL = interleukin; LIF = leukemia inhibitory factor; PlGF = placental-derived growth factor; M-CSF = macrophage colony-stimulating factor; SCF = stem cell factor; SDF-1 = stromal cell−derived factor; VEGF = vascular endothelial growth factor.

Western blot in membrane extracts (Fig. 3 A,B). Among endothelial GFs, VEGF-A/C and Ang-1 were abundantly secreted, Ang-2 and PLGF were detected in lower amounts, and VEGF-D was undetectable. As for stromal GFs, SDF-1 (CXCL12) secretion level was elevated (1147.7 ± 310.2 pg/mL/10^5 cells/24 hours) [9,10], BMP-2 was also

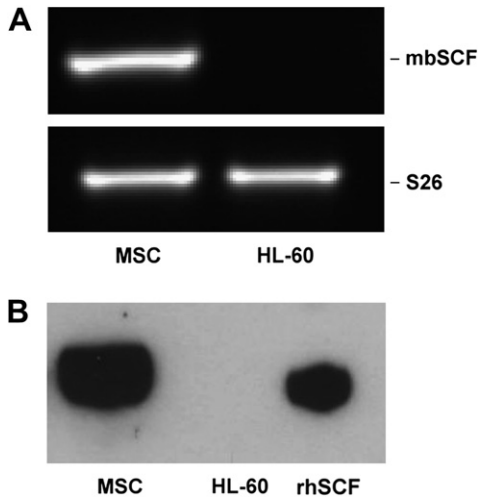

Figure 3. (**A**) Reverse transcriptase polymerase chain reaction for membrane-bound isoform of SCF (mbSCF) mRNA. HL-60 cell line was used as a negative control. S26 was used as endogenous control. (**B**) Western blot analysis of mbSCF protein in mesenchymal stromal cells. Human recombinant SCF (150 ng/lane) was used as positive control and HL-60 total protein extract was used as negative control. rhSCF =recombinant human stem cell factor.

significantly produced, while BMP-4, LIF, and insulin-like growth factor-1 (IGF-1) were undetectable. Our $CD146^+$ MSC cytokine secretion pattern provides additional informations over that reported for HSC-supporting mural cells [10].

Functional LTC assay

Because $CD146^+$ MSC phenotype is consistent with that of adventitial reticular cells composing HSC niches [9,10], we decided to evaluate their supportive function for hematopoiesis in vitro. $CD34^+$ cells were seeded at 3×10^3 on irradiated $CD146^+$MSCs or adherent cells from unseparated BM MNCs, showing a highly effective >2-log increase in the LTC colony output (Fig. 4A [28,29]).

The stromal function was further characterized by manipulating LTCs either with the KIT or VEGFR2/1 chemical inhibitors Imatinib [31] or SU-5416 [30], respectively. Both treatments similarly impaired the LTC colony output, indicating key roles for these two GF/GFR interactions for optimal MSCs supportive activity. SU5416 treatment of LTCs, at each concentration used, totally abrogated LTC colony output by week 6 (Fig. 4B), while Imatinib treatment caused a milder, although substantial, inhibition (Fig. 4B).

miRNA expression profile in chondrocyte differentiation

The miRNA expression profile was identified for two basal and two chondrogenic $CD146^+$ MSC samples by microarrays [32]. Statistical analysis revealed a specific modulation of 36 miRNAs during the chondrogenic differentiation process ($p < 0.05$). Twelve miRNAs were upregulated during differentiation, while 24 were downregulated, as indicated by the ratio of their expression value (Fig. 5A, Table 2). Northern blot analysis for the selected miRNAs, miR-23a, miR-26b, miR-214, and the Let-7a family confirmed the observed modulation (Fig. 5B). Putative targets of differentially expressed miRNAs were identified including genes involved in chondrogenic differentiation and tissue homeostasis. As shown in Table 2, the putative genes regulated by this set of miRNAs includes GF receptors (GFR) and cytokines (angiopoietin-1 [ANGPT1], insulin-like growth factor II receptor [IGF2R], transforming growth factor beta receptor [TGFBR], interleukin-6 [IL-6], fibroblast growth factor receptor [FGFR], placental growth factor [PGF], platelet-derived growth factor A [PDGFRA]), signal transduction mediators (mothers against decapentaplegic homolog 4 [SMAD4], mitogen-activated protein Kinase 1 [MAPK1], wingless-type MMTV integration site family member 1 [WNTP]), and molecules involved in the extracellular matrix remodeling (matrix metalloproteinases and collagens), all key regulators of human chondrogenesis.

We also performed enzyme-linked immunosorbent assay of angiopoietin-1, VEGF, and macrophage colony stimulating factor in $CD146^+$ MSC chondrogenic differentiation: these GFs emerged as putative targets for miR-204, miR-185/miR-199a-2-5p, and miR-214, respectively (Suppl.

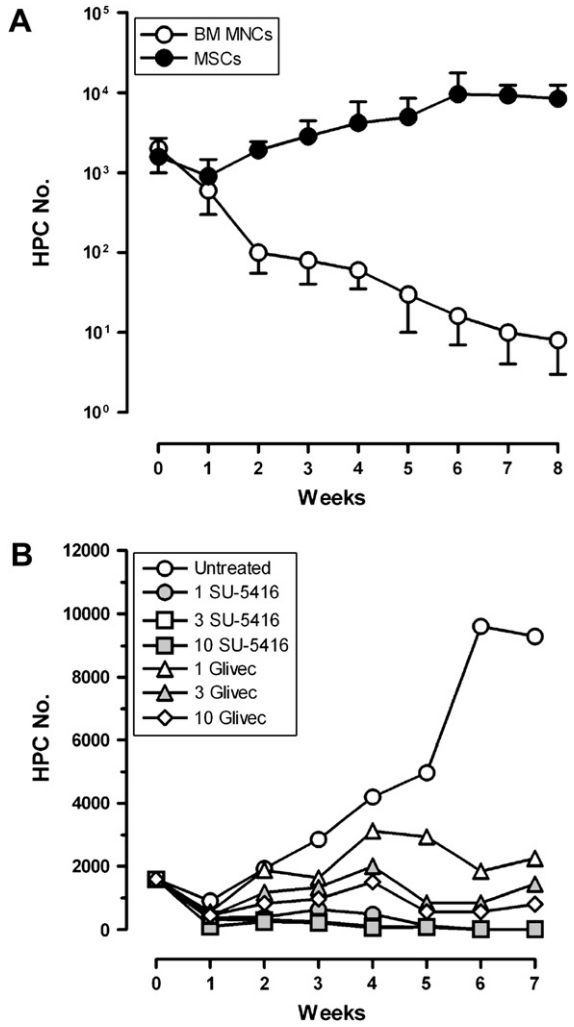

Figure 4. (**A**) Standard long-term culture (LTC). Progenitor cell output of 3×10^3 cord blood (CB) $CD34^+$ cells seeded on irradiated adherent bone marrow (BM) mononuclear cells (MNCs) or mesenchymal stromal cells (MSCs). Suspension cells were cloned weekly in multilineage semisolid media to evaluate hematopoietic progenitor cell (HPC) number. Values represent mean ± standard deviation of three experiments. (**B**) Effect of SU5416 on 3×10^3 CB $CD34^+$ cells seeded on irradiated MSCs. SU-5416 (VEGFR2/1 inhibitor) totally abrogated LTC progenitor output by week 6 at all concentrations (1, 3, and 10 μM), while control culture produced an elevated progenitor number (compare also with Fig. 4A). ST-1571 or GLIVEC (KIT inhibitor) treatment caused a similar but milder inhibition. Values represent mean ± standard error of mean from three experiments.

Fig. 3). Release of these GFs, was inversely correlated to the levels of the corresponding targeting miRNAs. Hypothetically, this pattern is compatible with an miRNA-mediated posttranscriptional regulation.

Discussion

Human BM hosts a double stem cell system, MSCs [1–3] and HSCs in postnatal age [28]. These two distinct stem cell populations arrange closely in specific architectural unities, the hematopoietic niches, ensuring hematopoietic and skeletal homeostasis. In the highly organized structure of the HSC niche, several signals are likely to take place [4–9]. Three types of HSC niches have been hypothesized, defined according to the HSC counterpart: the osteoblastic [4,5], the reticular stromal niche [6,9,10], and the vascular/sinusoidal endothelium niche [7,8]. The niches might play different roles in the regulation of HSC quiescence, proliferation, differentiation, and mobilization [4–10].

Our studies may provide a relatively simple, reproducible methodology for obtaining phenotypically homogeneous MSCs, expressing pivotal markers. Specifically, the lin^- BM MNC cell fraction was $CD34^+$ cell−depleted and expanded in clonal/low-density adherent MSC cultures. Removal of $CD34^+$ hematopoietic progenitors (HPCs) and endothelial cells, together with $CD14^+$ depletion, are critical to prevent MSC contamination with other cell types, particularly with monocytic progenitors endowed with some (2−4 weeks) clonogenic potential [41]. The resulting $CD146^+$ MSCs show coexpression at elevated intensity of stromal markers including CD90, GD2 [24], α-SMA [39] highly expressed and organized in fibers, CD140b and, to a lesser extent, CD140a [37,38]. Notably, $CD146^+$ MSC population represents only a minority of adherent BM MNCs [10,25]. MSCs also expressed the embryonic stem cell marker, SSEA-4 [23], whereas SSEA-1 was barely detectable [18]. The latter finding is possibly due to the fact that SSEA-1^+ MSCs represent a highly primitive stem cell population, generating also astrocytes and hepatocytes [18]. Finally, $CD146^+$ MSCs express hematopoietic markers, including several adhesion molecules [17,42], and endothelial antigens [25] at diverse intensity levels (see Results).

The antigen expression pattern was stable throughout the MSC lifespan for many of the analyzed markers (from P1 to P12), while most adhesion molecules decreased. Particularly, the multilineage CD146/$MCAM^+$ population was sharply reduced at P10 in parallel with a drop of the proliferation rate (see Results), the differentiation potential and the hematopoietic support function (data not shown). The expression of CD146, CD105, α-SMA, ALP in CD34/CD31/CD45-negative cells has been correlated with HSC niche-related pericytes surrounding endothelial sinusoids [10,43]. It has been also suggested that perivascular sites in microvessels represent the postnatal MSC niche [44], whose nature is to date far more elusive than the proposed HSC niches [4–9,41,45]. Interactions between very-late antigens (VLA-4 [CD29-CD49c]) and its ligand VCAM-1, (CD106)] may serve for both MSC/MSC anchoring and HPC/HSC homing [42]. The antigen expression analysis described here confirms and extends to 39 antigens the recently reported immunophenotype of self-renewing osteoprogenitors [10].

$CD146^+$ MSCs produce several GFs that may have an autocrine or a juxtacrine role at the HSC niche level. FL, IL-3, GM-CSF, and M-CSF were secreted, while SCF

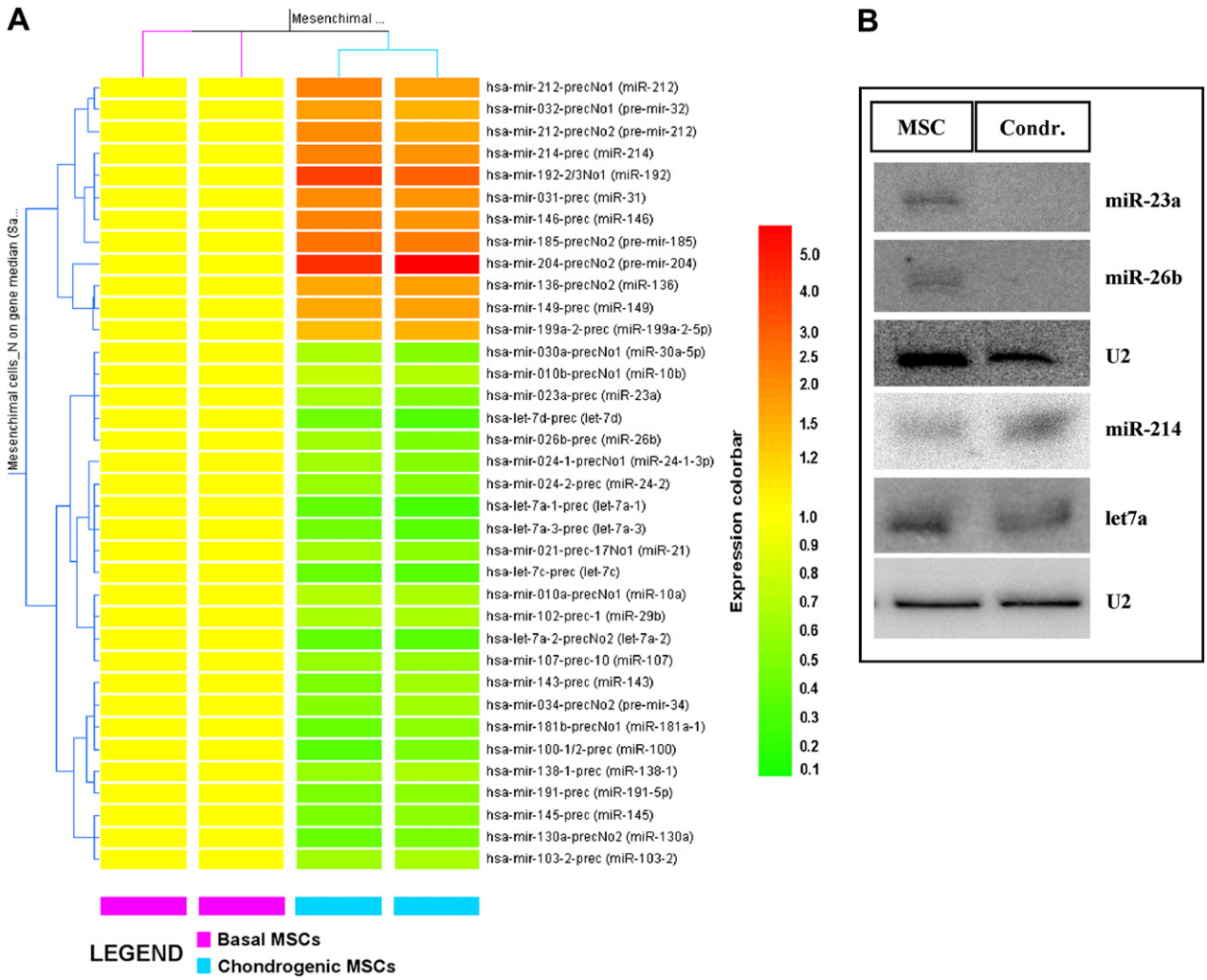

Figure 5. (**A**) Cluster analysis of chondrogenic MSCs differentiation based on 36 differentially expressed genes. A hierarchical cluster of four samples, based on 36 selected genes differentially expressed between chondrocyte differentiated and undifferentiated MCSs, generated a good separation of samples. A color-bar for gene expression values is shown on the right of the cluster: for each gene (rows), red indicates an expression value higher in chondrocytes than in MSCs; green shows a lower expression value. (**B**) Northern blot analysis of selected micro RNAs. U2 was used to normalize the total RNA loaded on each lane.

[10] was mostly produced in the membrane-bound form, confirming former reports on marrow stromal fibroblasts [46]. VEGF-A/C and Ang-1 [10] were abundantly secreted, Ang-2 and PLGF detected in lower amounts, and VEGF-D was undetectable. SDF-1 [9,10] secretion level was high, BMP-2 also abundant, but BMP-4, LIF, and IGF-1 were not detected. The role of angiogenic factors in regulating HSC is rapidly emerging [28,47,48], illustrated by the differential influence of VEGF-A [28], PLGF [47], and Ang-1 [10,48] on HSC fate [49]. Hypothetically, VEGF-A may also play an autocrine/paracrine role through PDGFR signaling [38]. While the role of Ang-2 in vascular remodeling is accepted [50,51], its effect on HSCs remains to be elucidated. As observed in endothelial cells [51], Ang-2 might function as antagonist or agonist of Tie-2 in HSCs. BMP-2 is a known osteogenic factor which can regulate the developmental program of human HSCs [52] or act synergistically with HGF on HPC differentiation [53]. The FL effect on human hematopoiesis is also multilevel [54]. SDF-1 regulates HSC and HPC mobilization and trafficking [9,10,11,55]. The membrane-bound isoform of SCF synergizes with soluble FL in supporting LTC initiating cells [56]. Furthermore, IL-3 [57] and GM-CSF [58] have pleiotropic effects on HPCs and mature cells. Finally, M-CSF, whose role on HPCs and mature cells is well-established [59–61], was also detected. Altogether, the combinatorial pattern of these HGFs and adhesion molecules, many of which act in synergy, may provide optimal hematopoietic support. In this regard, we report for the first time the use of a defined primary $CD146^+$ MSC population to establish LTCs. In 8-week $CD34^+$ cell LTC, MSCs provided a >2-log higher LTC colony output, as compared with standard

Table 2. MicroRNAs differentially expressed between differentiated chondrocyte and undifferentiated MSC and putative targets

MicroRNA	P-value	miRNA expression *Chondro/Control*	Symbol	Genbank	Map	**Putative targets**
pre-mir-204	0.0295	**4.97**	MIRN204		9q21.1	ANGPT1, IGF2R, BCL2, ESR1, CAV1,
miR-192	0.0135	**2.90**	MIRN192		11q13	RB1, CART1
pre-mir-185	0.00358	**2.18**	MIRN185		22q11.2	*VEGFA*, NFATC3, IGF2R, FURIN,
miR-146	0.00838	**1.78**	MIRN146A		5q34	TRAF6, RARB, SMAD4, CNTFR,
miR-214	0.0156	**1.78**	MIRN214	AJ550417	1q23.3	PGF, MAPK1, FGFR, CSF-1, CD47, CALMODULIN, CDK6,
miR-31	0.0125	**1.73**	MIRN31	AJ421753	9p21	CD71, HIF1AN, CALCR,
miR-212	0.0449	**1.72**	MIRN212	AJ550415	17p13.3	MAPK1, MMP16, COLQ,
pre-mir-212	0.0256	**1.62**	MIRN212	AJ550415	17p13.3	MAPK1, MMP16, COLQ,
miR-149	0.00576	**1.53**	MIRN149		2q37.3	PDGFRA, SP1, CD47, PGF, CD59, RORB, ADIPOR2,
miR-136	0.00716	**1.50**	MIRN136		14q32	ELK1, *LIFR*
pre-mir-32	0.0372	**1.44**	MIRN32	AJ421754	9q31.2	CD51, ITGA5, COL1A2, SMAD7, HAS3, NOTCH1, SMAD6, COL12A1, CDK6
miR-199a-2-5p	0.00237	**1.33**	MIRN199A2	AJ560756	1q24.3	ETS1, CAV1, JUNB, CTGF, HIF1A, *VEGFA*
miR-10b	0.0426	**0.76**	MIRN10B	AJ550395	2q31	FLT1, HAS3
miR-10a	0.00213	**0.72**	MIRN10A	AJ550394	17q21.3	FLT1, HAS3
miR-29b	0.00189	**0.70**	MIRN29B2	AF480543	1q32.2-32.3	COL3A1, COL5A3, COL11A1, COL5A1, COL1A2, COL4A5, *COL15A1, COL2A1, COL9A1, COL19A1, COL6A3, COL22A1, AKT3*
miR-103-2	0.00448	**0.67**	MIRN103-2	AF480501	2p13	FGF2, TGFBR3
miR-138-1	0.0195	**0.66**	MIRN138-1		3p21	RARA
miR-30a-5p	0.0429	**0.64**	MIRN30A	AF480535	6q12-13	RARB, CALCR, IL1A, CASP3, CBFB, ITGA5, SMAD1, IGF1R
miR-21	0.00994	**0.64**	MIRN21	AJ421741	17q23.2	STAT3, TGFBI, SMAD7
miR-107	0.00095	**0.63**	MIRN107	AF480505	10q23.31	FGF2, TGFBR3
miR-23a	0.0374	**0.63**	MIRN23A	AJ421743	19p13.2	Il-6R, MET, HS6ST2, TGFBR2, HOXD10, TGFA, TGFBR3, COL11A2, CCND1, IL-11
pre-mir-34	0.0337	**0.61**	MIRN34A	AJ550399	1p36.22	MET, PDGFRA, NOTCH, CALCR, COL12A1, CDK6, VCL, CCND1, WNT1
miR-24-1-3p	0.022	**0.61**	MIRN24-1	AJ421744	9q22.1	CALCR, PDGFRA, FLT1, MMP16, COL11A2, HAS3, IL1R1, MMP14, FGFR3,
miR-24-2	0.0149	**0.60**	MIRN24-2	AJ421745	19p13.2	CALCR, PDGFRA, FLT1, MMP16, COL11A2, HAS3, IL1R1, MMP14, FGFR3
miR-26b	0.0288	**0.60**	MIRN26B	AJ421748	2q35	SMAD1, COL10A1, COL1A2, SMAD4, LTBP1, COL11A1, ERBB4, IL-6, CBFB, COL12A1, CTGF
miR-143	0.0346	**0.60**	MIRN143		5q32-33	FGF1, CBFB, COL5A3, CTGF, LIFR, PDGFRA, IGFBP5, IL13RA
miR-145	0.00534	**0.57**	MIRN145		5q32-33	ERG, CDK6, BMPR2
miR-191-5p	0.0147	**0.57**	MIRN191		3p21	EGR1
miR-181a-1	0.029	**0.55**	MIRN213		1q31.2-q32.1	IL1A, PDGFRA, TNFSF11, SMAD7, RUNX1
miR-130a	0.00478	**0.50**	MIRN130A		11q12	RUNX3, SMAD5, WNT1, PDGFRA
miR-100	0.0272	**0.48**	MIRN100	AF480498	11q24.1	FGFR3, *RAC1*
let-7a-3	0.0122	**0.47**	MIRNLET7A3	AJ421726	22q13.3	TGFBR1, OSMR, COL1A2, COL3A1, COL14A1, IL13, CD61, COL1A1, GHR, COL4A2, FARP1, IL6, IL10, HAS2, MMP11, *CRTAP*,
let-7d	0.0335	**0.44**	MIRNLET7D	AJ421729	9q22.2	TGFBR1, OSMR, COL1A2, COL3A1, COL14A1, IL13, CD61, COL1A1, GHR, COL4A2, FARP1, IL6, IL10, HAS2, MMP11, *CRTAP*
let-7a-2	0.00128	**0.43**	MIRNLET7A2	AJ421725	11q24.2	TGFBR1, OSMR, COL1A2, COL3A1, COL14A1, IL13, CD61, COL1A1, GHR, COL4A2, FARP1, IL6, IL10, HAS2, MMP11, *CRTAP*
let-7c	0.00765	**0.43**	MIRNLET7C	AJ421728	21q11.2	TGFBR1, OSMR, COL1A2, COL3A1, COL14A1, IL13, CD61, COL1A1, GHR, COL4A2, FARP1, IL6, IL10, HAS2, MMP11, *CRTAP*
let-7a-1	0.0145	**0.39**	MIRNLET7A1	AJ421724	9q22.2	TGFBR1, OSMR, COL1A2, COL3A1, COL14A1, IL13, CD61, COL1A1, GHR, COL4A2, FARP1, IL6, IL10, HAS2, MMP11, *CRTAP*

Pre-miRs correspond to precursor microRNA, while miRs correspond to the mature product.

[a]Capital letters correspond to a gene that is predicted by the three algorithms. Italics are predicted by Target Scan and miRanda only.

adherent BM MNCs [29] stromal layers composed of randomly mixed cell types, including fibroblasts, adipocytes, macrophages, mesenchymal, and endothelial cells. Homogeneous CD146$^+$ MSC feeder layers may represent an in vitro surrogate model for studies on the HSC niche, or at least a significant improvement over standard LTC assays, allowing acquisition of data on HSC/MSC interactions to be validated in vivo.

MSC stromal function was further investigated manipulating LTCs either with the KIT or VEGFR2/1 chemical inhibitors Imatinib [31] or SU-5416 [30], respectively. Both treatments similarly impaired HPC output in LTCs, indicating key roles for these two GF/GFR interactions for optimal MSC/LTC-initiating cells cross-talk. Interestingly, SU-5416 treatment of CB CD34$^+$ cells totally abrogated HPC output by week 6, while Imatinib treatment caused a milder and slower inhibition.

In addition to functional hematopoietic support, CD146$^+$ MSCs exhibited canonical stem cell properties such as extended 12-week proliferation and multilineage potential toward chondrogenic, osteoblastic, and adipogenic differentiation.

To extend the molecular characterization of CD146$^+$ MSCs, the miRNA-expression profile was also analyzed by microarrays in both basal conditions and chondrogenic differentiation revealing 36 significantly modulated miRNAs. MiRNA expression profiles are characteristic of specific cell types, so they might represent reliable molecular markers specific to MSCs. Advances in miRNA profiling of MSCs and their terminally differentiated progeny will enable the delineation of standards for use in MSC quality control. Significantly, miRNA fingerprint in basal condition confirm and extend the recently published miRNA expression profile on undifferentiated MSCs [62], whereas the chondrogenesis data are novel. Bioinformatic analysis of the putative target genes for these miRNAs uncovered many fundamental cellular mediators of chondrogenic differentiation, as well as tissue maintenance, including GFs (IL-6, PGF, ANGPT1, CSF-1, FGF) and GFRs (TGFBR, PDGFRA, IGF2R, FGFR). Therefore, the present work provides the basis for more detailed investigation at the level of single miRNAs and their putative targets, in order to unveil miR-based regulatory pathways in normal human chondrogenesis. Hypothetically, this study might contribute to the future development of novel therapeutic approaches in hemophiliac's arthropathy.

A similar approach has been applied to studies on hematopoiesis with considerable success [33,63,64]. Ongoing studies aim to expand our initial observations to osteogenic and adipogenic differentiation.

Additionally, a CD146$^+$ MSC population could be advantageous for in vivo regenerative therapy studies [1,15,18–22].

In conclusion, the availability of a phenotypically homogeneous CD146$^+$ MSC population, meeting the required MSC definition criteria [65,66], will allow to obtain consistent results in both basic and clinical studies, thus facilitating progress in this research area.

Acknowledgments

We thank E. Pelosi, P. Di Matteo, and A. D'Angiò for technical assistance, M. Fontana, D. Marinelli and A. Zito for editorial assistance and graphics. We also thank L.M. Starnes, P. Bianco and A. Santoni for critical reading of the manuscript. This work was supported by Italy-USA Oncology Program on microRNAs and antisense sequences (to C.P.) and FIRB 2001 Grant RBNE01SP72-004 (to M.V.)

References

1. Bianco P, Robey PG. Stem cells in tissue engineering. Nature. 2001; 414:118–121.
2. Pittenger MF, Mackay AM, Beck SC, et al. Multilineage potential of adult human mesenchymal stem cells. Science. 1999;284:143–147.
3. Prockop DJ. Marrow stem cells as stem cells for non-hematopoietic tissues. Science. 1997;276:71–74.
4. Zhang J, Niu C, Ye L, Huang H, et al. Identification of the haematopoietic stem cell niche and control of the niche size. Nature. 2003;425: 836–841.
5. Calvi LM, Adams GB, Welbrecht KW, et al. Osteoblastic cells regulate the haematopoietic stem cell niche. Nature. 2003;425:841–846.
6. Kuznetsov SA, Riminucci M, Ziran N, et al. The interplay of osteogenesis and hematopoiesis: expression of a constitutively active PTH/PTHrP receptor in osteogenic cells perturbs the establishment of hematopoiesis in bone and of skeletal stem cells in the bone marrow. J Cell Biol. 2004;167:1113–1122.
7. Li W, Johnson SA, Shelley WC, et al. Hematopoietic stem cell repopulating ability can be maintained in vitro by some primary endothelial cells. Exp Hematol. 2004;32:1226–1237.
8. Kiel MJ, Yalmaz OH, Iwashita T, et al. SLAM family receptors distinguish hematopoietic stem and progenitor cells and reveal endothelial niches for stem cells. Cell. 2005;121:1109–1121.
9. Sugiyama T, Kohara H, Noda M, et al. Maintenance of the hematopoietic stem cell pool by CXCL12-CXCR4 chemokine signaling in bone marrow stromal cell niches. Immunity. 2006;25:977–988.
10. Sacchetti B, Funari A, Michienzi S, et al. Self-renewing osteoprogenitors in bone marrow sinusoids can organize a hematopoietic microenvironment. Cell. 2007;131:324–336.
11. Pelosi E, Valtieri M, Coppola S, et al. Identification of the hemangioblast in postnatal life. Blood. 2002;100:3203–3207.
12. da Silva Meirelles L, Chagastelles PC, Nardi B. Mesenchymal stem cells reside in virtually all post-natal organs and tissues. J Cell Sci. 2006;119:2204–2213.
13. Wagner W, Wein F, Seckinger A. Comparative characteristics of mesenchymal stem cells from human bone marrow, adipose tissue, and umbilical cord blood. Exp Hematol. 2005;33:1402–1416.
14. Kassis I, Zangi L, Rivkin R, et al. Isolation of mesenchymal stem cells from G-CSF-mobilized human peripheral blood using fibrin microbeads. Bone Marrow Transplant. 2006;37:967–976.
15. Mansilla E, Marin GH, Drago H, et al. Bloodstream cells phenotypically identical to human mesenchymal bone marrow stem cells circulate in large amounts under the influence of acute large skin damage: new evidence for their use in regenerative medicine. Transplant Proc. 2006;38:967–969.
16. Jiang Y, Jahagirdar BN, Reinhardt RL, et al. Pluripotency of mesenchymal stem cells derived from adult marrow. Nature. 2002;418:41–49.

17. Yin T, Li L. The stem cell niches in bone. J Clin Invest. 2006;116: 1195–1201.
18. Anjos-Afonso F, Bonnet D. Nonhematopoietic/endothelial SSEA-1+ cells define the most primitive progenitors in the adult murine bone marrow mesenchymal compartment. Blood. 2007;109:1298–1306.
19. Seruya M, Shah A, Pedrotty D, et al. Clonal population of adult stem cells: life span and differentiation potential. Cell Transplant. 2004;13: 93–101.
20. Pittenger MF, Martin BJ. Mesenchymal stem cells and their potential as cardiac therapeutics. Circulation Res. 2004;95:9–20.
21. Wenisch S, Trinkaus K, Hild A, et al. Immunochemical, ultra structural and electrophysiological investigations of bone-derived stem cells in the course of neuronal differentiation. Bone. 2006;38:911–921.
22. Ong SY, Dai H, Leong KW. Inducing hepatic differentiation of human mesenchymal stem cells in pellet culture. Biomaterials. 2006;22: 4087–4097.
23. Gang EJ, Bosnakovski D, Figueiredo CA, et al. SSEA-4 identifies mesenchymal stem cells from bone marrow. Blood. 2007;109:1743–1751.
24. Martinez C, Hofmann TJ, Marino R, et al. Human bone marrow stromal cells express the neural ganglioside GD2: a novel surface marker for the identification of MSCs. Blood. 2007;109:4245–4248.
25. Baksh D, Yao R, Tuan RS. Comparison of proliferative and multilineage differentiation potential of human mesenchymal stem cells derived from umbilical cord and bone marrow. Stem Cells. 2007;25:1384–1392.
26. Bartel DP. MicroRNAs: genomics, biogenesis, mechanism, and function. Cell. 2004;116:281–297.
27. Kloosterman WP, Plasterk RH. The diverse functions of microRNAs in animal development and disease. Dev Cell. 2006;11:441–450.
28. Ziegler BL, Valtieri M, Almeida Porada G, et al. KDR receptor: a key marker defining hematopoietic stem cells. Science. 1999; 285:1553.
29. Valtieri M, Schiro R, Chelucci C, et al. Efficient transfer of selectable and membrane reporter genes in hematopoietic progenitor and stem cells purified from human peripheral blood. Cancer Res. 1994;54: 4398–4404.
30. Ye C, Sweeny D, Sukbuntherng J, Zhang Q, et al. Distribution, metabolism, and excretion of the anti-angiogenic compound SU5416. Toxicol In Vitro. 2006;20:154–162.
31. Rubin BP, Heinrich MC, Corless CL. Gastrointestinal stromal tumor. Lancet. 2007;369:1731–1741.
32. Liu CG, Calin GA, Meloon B, et al. An oligonucleotide microchip for genome-wide microRNA profiling in human and mouse tissues. Proc Natl Acad Sci U S A. 2004;101:9740–9744.
33. Felli N, Fontana L, Pelosi E, et al. MicroRNAs 221 and 222 inhibit normal erythropoiesis and erytholeukemic cell growth via kit receptor down-modulation. Proc Natl Acad Sci U S A. 2005;102:18081–18086.
34. Lewis BP, Shih IH, Jones-Rhoades MW, et al. Prediction of mammalian microRNA targets. Cell. 2003;115:787–798.
35. Krek A, Grun D, Poy MN, et al. Combinatorial microRNA target prediction. Nat Genet. 2005;37:495–500.
36. John B, Enright AJ, Aravin A, et al. Human microRNA targets. PloS Biol. 2004;2:e363.
37. Schwab KE, Gargett CE. Co-expression of two perivascular cell markers isolates mesenchymal stem-like cells from human endometrium. Hum Reprod. 2007;22:2903–2911.
38. Ball SG, Shuttleworth A, Kielty CM. Vascular endothelial growth factor can signal through platelet-derived growth factor receptors. J Cell Biol. 2007;177:489–500.
39. Wang D, Park JS, Chu JSF, et al. Proteomic profiling of bone marrow mesenchymal stem cells upon transforming growth factor β stimulation. J Biol Chem. 2004;279:43725–43734.
40. Cristofalo VJ, Volker C, Francis MK, et al. Age-dependent modifications of gene expression in human fibroblasts. Crit Rev Eukaryot Gene Expr. 1998;8:43–80.
41. Metcalf D. Concise review: hematopoietic stem cells and tissue stem cells: current concepts and unanswered questions. Stem Cells. 2007; 25:2390–2395. Epub 2007 Aug 9.
42. Verfaille CM. Adhesion receptors as regulators of the hematopoietic process. Blood. 1998;92:2609–2612.
43. Li Q, Bischoff J, Mulliken JB, Olsen BR. Differential expression of CD146 in tissues and endothelial cells derived from infantile haemangioma and normal human skin. J Pathol. 2003;201:296–302.
44. Shi S, Gronthos S. Perivascular niche of postnatal mesenchymal stem cells in human bone marrow and dental pulp. J Bone Miner Res. 2003; 18:696–704.
45. Miller FD. Riding the waves: neural and nonneural origins for mesenchimal stem cells. Cell Stem Cell. 2007;1:129–130.
46. Linenberger ML, Jacobson FW, Bennett LG, et al. Stem cell factor production by human marrow stromal fibroblasts. Exp Hematol. 1995;23:1104–1114.
47. Hattori K, Heissig B, Wu Y, et al. Placental growth factor reconstitutes hematopoiesis by recruiting VEGFR1(+) stem cells from bone marrow microenvironment. Nat Med. 2002;8:841–849.
48. Arai F, Hirao A, Ohmura M, et al. Tie2/angiopoietin-1 signalling regulates hematopoietic stem cell quiescence in the bone marrow niche. Cell. 2004;118:149–161.
49. Han W, Yu Y, Liu XY. Local signals in stem cell-based bone marrow regeneration. Cell Res. 2006;16:189–195.
50. Roy H, Bhardwaj S, Yla-Herttuala S. Biology of vascular endothelial growth factors. FEBS Lett. 2006;580:2279–2287.
51. Eklund L, Olsen BR. Tie receptors and their angiopoietin ligands are context-dependent regulators of vascular remodelling. Exp Cell Res. 2006;312:630–641.
52. Bhatia M, Bonnet D, Wu D, et al. Bone morphogenetic proteins regulate the developmental program of human hematopoietic stem cells. J Exp Med. 1999;189:1139–1148.
53. Detmer K, Walker AN. Bone morphogenetic proteins act synergistically with hematopoietic cytokines in the differentiation of hematopoietic progenitors. Cytokine. 2002;17:36–42.
54. Gabbianelli M, Pelosi E, Montesoro E, et al. Multi-level effects of flt3 ligand on human hematopoiesis: expansion of putative stem cells and proliferation of granulomonocytic progenitors/monocytic precursors. Blood. 1995;86:1661–1670.
55. Liles WC, Broxmeyer HE, Rodger E, et al. Mobilization of hematopoietic progenitor cells in healthy volunteers by AMD3100, a CXCR4 antagonist. Blood. 2003;102:2728–2730.
56. Slanicka Krieger M, Nissen C, Manz CY, et al. The membrane-bound isoform of stem cell factor synergizes with soluble flt3 ligand in supporting early hematopoietic cells in long-term cultures of normal and aplastic anemia bone marrow. Exp Hematol. 1998;26:365–373.
57. Scott CL, Robb L, Papaevangeliou B, et al. Reassessment of interactions between hematopoietic receptors using common beta-chain and inteleukin-3-specific receptor beta-chain-null cells: no evidence of functional interactions with receptor for erythropoietin, granulocyte colony-stimulating factor, or stem cell factor. Blood. 2000;96:1588–1590.
58. Fleetwood AJ, Cook AD, Hamilton JA. Functions of granulocyte-macrophage colony-stimulating factor. Crit Rev Immunol. 2005;25: 405–428.
59. Chitu V, Stanley ER. Colony-simulating factor-1 in immunity and inflammation. Curr Opin Immunol. 2006;18:39–48.
60. Nakano T. In vitro development of hematopoietic system from mouse embryonic stem cells: a new approach for embryonic hematopoiesis. Int J Hematol. 1996;65:1–8.
61. Takakura N, Kodama H, Nishikawa S, Nishikawa S. Preferential proliferation of colony-forming units in a chemically defined condition

with a macrophage colony-stimulating factor-negative stromal cell clone. J Exp Med. 1996;184:2301–2309.
62. Greco SJ, Rameshwar P. MicroRNAs regulate synthesis of the neurotransmitter substance P in human mesenchymal stem cells-derived neuronal cells. Proc Natl Acad Sci U S A. 2007;104:15484–15489.
63. Fontana L, Pelosi E, Greco P, et al. The microRNAs 17-5p/-20a/106a function as a master gene complex controlling monocytopoiesis through AML1 targeting. Nat Cell Biol. 2007;9:775–787.
64. Fazi F, Rosa A, Fatica A, et al. A minicircuitry comprised of microRNA-223 and transcription factor NFI-A and C/EBPalpha regulates human granulopoiesis. Cell. 2005;5:819–831.
65. Dominici M, Le Blanc K, Mueller I, et al. Minimal criteria for defining multipotent mesenchymal stromal cells. Cytotherapy. 2006; 8:315–317.
66. Delorme B, Ringe J, Gallay N, et al. Specific plasma membrane protein phenotype of culture-amplified and native human bone marrow mesenchymal stem cells. Blood. 2008;111:2631–2635. Epub 2007 Dec 17.

Supplementary data associated with this article can be found, in the online version, at doi:10.1016/j.exphem.2008.03.004.